cosmetics

MDPI

Article

Regenerative and Dermal Wound Healing Activities of Bioactive Octapeptide

Shan Lakmal Edirisinghe, Chamilani Nikapitiya and Mahanama De Zoysa *

College of Veterinary Medicine and Research Institute of Veterinary Medicine, Chungnam National University, Daejeon 34134, Republic of Korea
* Correspondence: mahanama@cnu.ac.kr

Abstract

Cosmeceutical peptides (CPs), which modulate various biological activities, including skin regeneration and wound healing, have emerged as promising agents in skincare. In this study, we investigated the regenerative and wound healing potential of a short peptide, CP-02 (sequence CDARSDAR), using human dermal fibroblast cells (HDFs) in vitro and a zebrafish model in vivo. In HDFs, CP-02 treatment at concentrations of 50, 100, and 200 µg/mL significantly accelerated wound closure in a dose-dependent manner ($p < 0.05$) and upregulated the mRNA expression of *CCND1*, *MYC*, *FGF2*, *EFG*, and *IL-8* at 12 h post-treatment. In amputated zebrafish larvae, exposure to CP-02 (5 µg/mL) for 72 h significantly increased fin regeneration, with a fin area of 3.5 mm^2 and fin-fold length of 0.2 mm, compared with those in controls (2 mm^2 and 0.07 mm, respectively). Intramuscular administration of CP-02 significantly improved the healing rates in wounded adult zebrafish to 58% and 76% on 12 and 16 days post wounding (dpw), respectively, compared with the vehicle (35% and 44%, respectively). Histological analysis (H&E staining) revealed reduced inflammatory cell infiltration, complete granulation, and re-epithelialization in the CP-02-treated tissues at 12 dpw. Furthermore, mRNA expression levels of *tnf-α*, *il-1β*, *tgfb1*, *mmp9*, *mmp13*, and *timp2b* were elevated in the CP-02 group at 4 dpw, whereas those of pro-fibrotic mediators, including *acta2*, *ctgfb*, *cdh1*, and *col9a3* reduced in muscle tissue on 12 dpw. Collectively these findings demonstrate that CP-02 promotes effective, scar-reducing regeneration and wound healing, highlighting its strong potential as a therapeutic peptide for future skincare and cosmeceutical applications.

Keywords: cosmeceutical peptides; regeneration; wound healing; zebrafish

Check for updates

Academic Editor: Bryan Fuller

Received: 14 August 2025
Revised: 3 December 2025
Accepted: 24 December 2025
Published: 13 January 2026

Correction Statement: This article has been republished with a minor change. The change does not affect the scientific content of the article and further details are available within the backmatter of the website version of this article.

Copyright: © 2026 by the authors. Licensee MDPI, Basel, Switzerland. This article is an open access article distributed under the terms and conditions of the Creative Commons Attribution (CC BY) license.

1. Introduction

Peptides are increasingly recognized as multifunctional agents in various biopharmaceutical and cosmeceutical formulations, owing to their capability to modulate diverse biological activities, including innate immune responses and the restoration of skin barrier functions [1,2]. Numerous studies have demonstrated that specifically designed endogenous peptides can promote wound healing by promoting angiogenesis and re-epithelialization in in vitro and in vivo models [1–3].

Healing of skin wounds is a complex and dynamic biological process that involves various cell types, signaling pathways, growth factors, and inflammatory mediators [4,5]. This process progresses through four phases: hemostasis, inflammation, proliferation, and remodeling [6]. Synthetic peptides have shown great potential in supporting these processes by accelerating hemostasis [7], promoting cell migration and proliferation, and

enhancing macrophage recruitment on wound sites [8]. Moreover, synthetic peptides promote the production of endogenous wound healing factors and growth mediators essential for tissue repair [8].

In recent years, growing interest from the biopharmaceutical and skin care industries has focused on cosmeceutical peptides (CPs) for their therapeutic benefits, such as anti-aging, anti-wrinkle effects, skin regeneration, and wound healing, as well as the inhibition of melanogenesis [1]. Owing to their stability, ease of synthesis, and biological versatility, CPs have been widely incorporated into various skincare formulations. Furthermore, short peptides exhibit structural diversity and conformational flexibility, which promote their involvement in a wide range of interactions with specific membrane receptors associated with healing and regenerative processes. Despite their promising therapeutic potential, challenges such as limited stability, receptor specificity, and skin penetration persist, prompting the continued development of improved peptides through structural and chemical modifications.

CPs can be broadly classified into four functional groups: signaling peptides, carrier peptides, neurotransmitter-inhibiting peptides, and enzyme-inhibiting peptides [9]. Signal peptides stimulate specific cellular pathways to enhance collagen synthesis and tissue regeneration [9]. Carrier peptides facilitate the delivery of trace elements to the skin, thereby supporting enzymatic functions and repair processes [10]. Neurotransmitter-inhibiting peptides reduce muscle contractions associated with visible signs of aging, while enzyme-inhibiting peptides function as antioxidants or anti-inflammatory agents to protect against skin disorders such as sunburn [9]. Many modern cosmeceutical formulations contain CPs with one or more of these biological activities [9]. However, only a few studies have explored the dual role of short peptides in wound healing and scar-reduction [11].

To address this gap, the present study aimed to synthesize a short peptide and evaluate its potential tissue regeneration and wound healing through comprehensive in vitro and in vivo assays. The findings of this study provide valuable insight into therapeutic potential of short peptides and may guide their future applications in skin care formulations and wound healing strategies.

2. Materials and Methods

2.1. Design and Synthesis of CP-02

The CP-02 peptide (sequence: CDARSDAR) was synthetically produced and commercially supplied by ANYGEN Biotechnology Co., Ltd. (Gwangju, Republic of Korea). The final purity of CP-02 used to determine biological activities was >95.8%, as determined by reverse-phase high performance liquid chromatography (RP-HPLC) analysis using SHIMADZU HPLC LabSolutions (Shimadzu, Inc., Kyoto, Japan). Owing to its high hydrophilicity. CP-02 was dissolved in nuclease-free (NF) water to prepare desired concentrations for each set of experiment conditions.

2.2. Cell Culture and Cytotoxicity Studies of CP-02

The cytotoxicity of CP-02 was evaluated using the 3-(4,5-dimethylthiazol-2-yl)-2,5-diphenyltetrazolium bromide (MTT) reduction assay. Briefly, HDFs (ATCC PCS-201-010™, Manassas, VA, USA) were cultured in low-serum fibroblast basal medium (Manassas, VA, USA) at 37 °C in a humidified atmosphere containing 5% CO_2. For the assay, HDFs were seeded in 96-well microplates at a density of 2.5×10^5 cells per well and incubated for 12 h under the same conditions. Cells were then treated with varying concentrations of CP-02 (12.5–250 μg/mL) and incubated for 24 h. Subsequently, the medium was replaced with fresh medium containing 10 μL of MTT (5 mg/mL; Sigma-Aldrich, St. Louis, MO, USA) and incubated for 4 h to allow for formazan crystal formation. The resulting crystals were

dissolved in 50 µL of dimethyl sulfoxide (DMSO) and absorbance was measured at 570 nm using a microplate spectrophotometer (Bio-Rad Laboratories, Inc., Hercules, CA, USA). Untreated cells (0 µg/mL CP-02) served as the control and were considered 100% viable.

2.3. In Vitro Wound Healing and mRNA Expression upon CP-02 Treatment

In vitro wound healing assay was performed as previously described [12], with minor modifications. Briefly, 70 µL of HDF cells (2×10^5 cells/mL) was seeded into each well of culture-insert 2 well (ibidi, Munich, Germany) and incubated for 24 h at 37 °C in a humidified atmosphere containing 5% CO_2. After cell attachment, the insert was gently removed to create a uniform cell-free gap of approximately 500 µm. A total of 2 mL of fresh culture medium containing CP-02 at concentrations of 50 and 200 µg/mL was added, and cells were incubated under the same conditions. Wound closure was monitored by capturing images at 0, 12, 24, and 36 h using an inverted light microscope (DMi8, Leica, Wetzlar, Germany). The experiment was performed in triplicate (n = 3), and wound closure was quantified using ImageJ software (ImageJ, ver. 1.6, Bethesda, MD, USA) by normalizing the remaining wound area to the initial (0 h) gap size. For mRNA expression analysis, HDFs were seeded in 6-well plates at a density of 2×10^5 cells/mL and incubated for 12 h at 37 °C in 5% CO_2 atmosphere. The medium was then replaced with fresh medium containing 100 and 200 µg/mL of CP-02. After 12 and 24 h of treatment, the cells were washed twice with phosphate-buffered saline (PBS), collected, and stored at −80 °C until RNA extraction.

2.4. Maintenance of Larvae and Adult Zebrafish

All zebrafish experiments were conducted in accordance with the guidelines and regulations approved by the Animal Ethics Committee of Chungnam National University. Wild-type (AB strain) adult zebrafish were maintained under laboratory conditions with a 14 h light/10 h dark photoperiod. Water quality parameters were monitored and maintained as follows: dissolved oxygen > 6 mg/L, conductivity 500–600 µS, nitrate < 30 µg/L, and nitrite < 0.01 mg/mL. Male and female zebrafish (6 months old) were placed in breeding tanks, and fertilized embryos were collected following natural spawning. The embryos were incubated at 28 ± 0.5 °C in embryonic medium (EM) until hatching.

2.5. In Vivo Larval Toxicity and Regenerative Activity of CP-02

The in vivo toxicity assays were conducted as previously described [13], with slight modifications. Briefly, zebrafish embryos at 2 h post-fertilization (hpf) were exposed to various concentrations of CP-02 (0–7.5 µg/mL) in 6-well plates, with each concentration tested in triplicate. Based on the observed toxicity profiles, two non-toxic concentrations were selected for subsequent evaluation of regenerative activity. At 4 days post fertilization (4 dpf), larvae were anesthetized using 0.05% (w/v) tricaine (Sigma-Aldrich, St Louis, MO, USA), and the caudal fin was amputated posterior to the notochord following the protocol described by Edirisinghe et al. [12]. Immediately post-amputation (0 h post-amputation, hpa), larvae were imaged to document the initial wound area. Subsequently, they were transferred individually into wells of a 96-well plate containing either control medium or medium supplemented with CP-02 at concentrations of 2.5 and 5 µg/mL. Images were captured at 24, 48, and 72 hpa to monitor regenerative progress. Fin regeneration was assessed by measuring the regrown fin area and fin fold length using ImageJ software (version 1.6, Bethesda, MD, USA) in a blinded manner.

2.6. In Vivo Wound Healing of CP-02

One hundred and twenty AB adult male zebrafish (average body weight 0.45 ± 0.05 g) were maintained in 10 L tanks and randomly assigned to three groups: vehicle, CP-02, and

Epidermal Growth Factor (EGF). All fish were acclimatized for one week before initiating the wound healing experiment. Full-thickness skin wounds (2 mm in diameter) were created on the left flank of each fish, anterior to the anal and dorsal fins, using a sterile disposable biopsy punch (Kai Medical, Gifu, Japan). On 2-day post wounding (dpw), 12 fish from each group with uniformly sized wounds were selected from each group and individually housed in 500 mL tanks. The CP-02 group received four intramuscular (I.M.) injections of CP-02 (1 µg/fish in 2 µL per dose): one pre-treatment dose administered 24 h before wounding, followed by three post-wounding doses on 3, 7, and 12 dpw. Injections were delivered into the dorsal muscle on the left side of the fish. Each fish in the positive control group received 2 ng human EGF (2 µL per dose; R&D Systems, Minneapolis, MN, USA) on the same dosing schedule, while the vehicle group received equivalent volumes of normal NF water. Wound healing progression was monitored on 2, 4, 8, 12, and 16 dpw using a digital camera (KL300 LED; Leica) connected to a stereo-microscope (S8 APO; Leica; Wetzlar, Germany). The wound area was quantified using ImageJ software (ver. 1.6) based on pigmentation differences and changes in skin color intensity (from pale to dark), as described by Edirisinghe et al. [12]. The results were expressed as percentage healing profile and wound healing rate (WHR) normalized to the initial wound size on 2 dpw.

2.7. Histological and Transcriptional Analysis of Skin Regeneration

Given the temporal dynamics of zebrafish wound healing, granulation tissue formation is expected to peak around 7 dpw, with tissue remodeling becoming prominent by 12 dpw. Therefore, histological assessments were performed at these two times. Six fish from each group (vehicle, CP-02, EGF) were anesthetized with an overdose of Tricaine on 7 and 12 dpw. The wounded muscle area was surgically excised, soaked in PBS, and fixed in 10% neutral buffered formalin (10% NBF) for 21 days. Tissues were then rinsed for 6 h under tap water to remove residual fixatives and processed using a semi-enclosed benchtop tissue processor (TP1020; Leica). Following dehydration and clearing, tissues were embedded in paraffin wax at EG1150 Tissue Embedding Center (Leica), sectioned into 4 µm thick slices using a microtome (RM2125; Leica), and stained with hematoxylin–eosin (H&E) staining using a H&E staining kit (cat # ab245880; Abcam, Cambridge, UK) following the manufacturer's instructions. Finally, stained tissue sections were visualized and imaged using a digital camera (DCF450-C; Leica) connected to a microscope (DM 3000 LED; Leica). For transcriptional analysis, wounded muscle tissues from the same sampling time points (7 and 12 dpw) and groups were harvested, snap-frozen in liquid nitrogen, and stored at −80 °C until RNA extraction.

2.8. Quantitative Real Time-PCR Analysis

Total RNA was extracted from cultured HDFs and wounded zebrafish muscle tissues using TRIzol® reagent (Invitrogen, Waltham, MA, USA), following the manufacturer's protocol. RNA concentration and purity were assessed using a NanoDrop One spectrophotometer (Thermo Scientific, Waltham, MA, USA), as described previously Rajapaksha et al. [14]. First-strand cDNA synthesis was performed using 2.5 µg of total RNA with the PrimeScript™ 1st Strand cDNA Synthesis Kit (TaKaRa, Bio Inc., Shiga, Japan), according to the manufacturer's instructions. The synthesized cDNA was diluted 40-fold and stored at –20 °C until further use. In HDFs, the expression of genes associated with cell cycle regulation (*CCND1*, *CDKN1B*, and *MYC*), growth factors (*FGF2*, *EGF*, *TGFB1*, and *VEGFA*), inflammation (*IL8*), and oxidative stress response (*CAT*) was analyzed. In zebrafish wound tissues, the expression profiling included pro- and anti-inflammatory markers (*tnfa*, *il1b*, and *il10*), extracellular matrix (*ECM*) remodeling (*tgfb1*, *mmp9*, *mmp13*, and *timp2b*), and excess scar production (*acta2*, *ctgfb*, *cdh1*, and *col9a3*)-related genes. Gene-specific primers

(Supplementary Table S1) were used for quantitative real-time PCR conducted on a Thermal Cycler Dice Real-Time System (TaKaRa, Bio Inc., Shiga, Japan), as previously reported [12]. Each 10 µL reaction contained 3 µL of diluted cDNA, 1 µL of each forward and reverse primer (10 µM), and 5 µL of TB Green® Premix Ex Taq™ II (TaKaRa, Japan). The amplification protocol followed a standard three-step thermal cycling profile with gene-specific annealing temperatures. The relative mRNA expression level was determined using the $2^{-\Delta\Delta Ct}$ method [15], using *GAPDH* and β-actin as the internal controls for HDFs and zebrafish samples, respectively.

2.9. Statistical Analysis

All the statistical analyses were conducted using GraphPad Prism software, version 5 (GraphPad Software Inc. San Diego, CA, USA). Data were analyzed using one-way/or two-way analysis of variance (ANOVA) to determine significant differences among experimental groups and time points. A p-value ≤ 0.05 was considered statistically significant. As indicated, data are presented as the mean ± standard deviation (SD) from duplicate or triplicate experiments.

3. Results

3.1. Characterization and Physiochemical Properties of CP-02

The molecular weight of synthesized CP-02 was 892.9 Da with 95.8% final purity. (Supplementary Figure S1).

3.2. In Vitro Dose Optimization of CP-02 for Treating HDFs

The MTT colorimetric assay results revealed that the percent cell viability was significantly increased in CP-02-treated (100 to 250 µg/mL) HDFs compared with the untreated control group ($p < 0.05$; Supplementary Figure S2A). However, cell viability notably declined at concentrations above 250 µg/mL, with the half-maximal inhibitory concentration (IC_{50}) of CP-02 determined to be 322 µg/mL (Supplementary Figure S2B). Although higher CP-02 concentrations did not induce apparent morphological alterations in HDFs, both cell proliferation and migration were substantially suppressed at concentrations above 250 µg/mL. Based on these cytotoxicity data, CP-02 concentrations of 50, 100, and 200 µg/mL were selected for subsequent in vitro wound healing assays.

3.3. CP-02 Enhances HDF Migration and In Vitro Wound Healing

Evaluation of wound closure, based on the reduction in the cell-free gap at 6, 12, 24, and 36 h post treatment (hpt), demonstrated that CP-02 treatment significantly reduced the wound area in a concentration-dependent manner (Figure 1A). Specifically, treatment with 50 and 100 µg/mL CP-02 led to a significant reduction in the wound area at 12 (85.6% and 80.0%, respectively; $p < 0.05$), 24 (70.0% and 54.4%, respectively; $p < 0.01$), and 36 h (38.2% and 17.3%, respectively; $p < 0.001$) compared with those in control group at these respective time points. The highest dose, 200 µg/mL, produced the most pronounced wound closure, significantly reducing the open wound area at all time points ($p < 0.001$). These findings indicate that CP-02 promotes HDF migration and enhances in vitro wound healing in a dose-dependent manner.

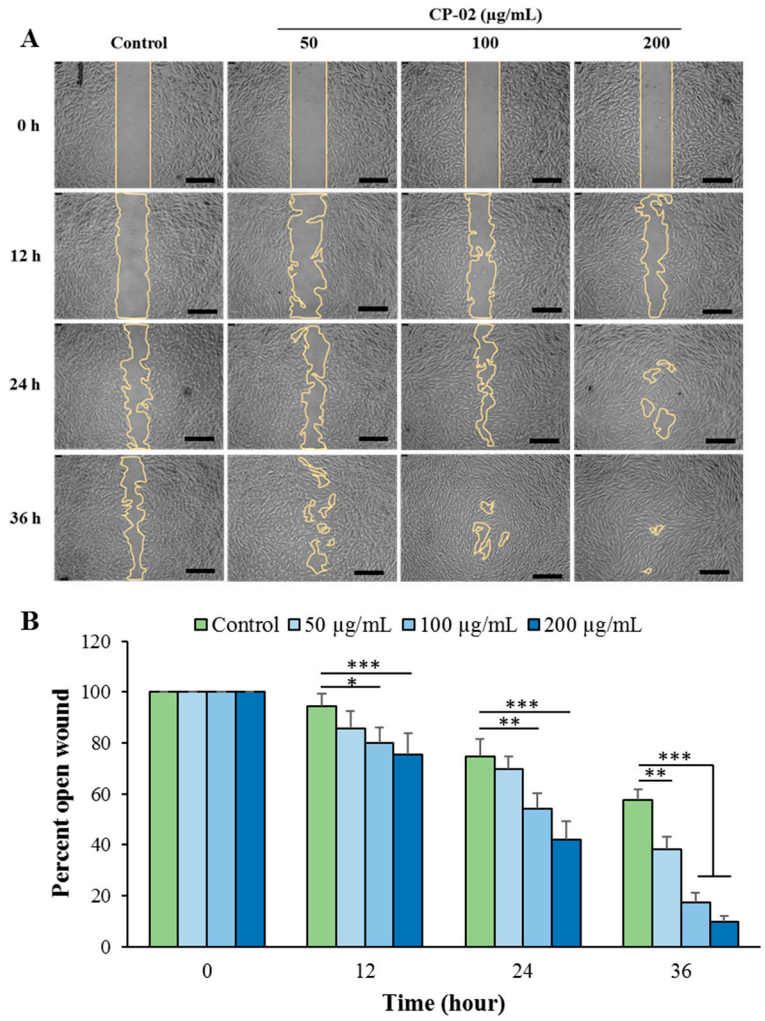

Figure 1. Effect of CP-02 on in vitro cell migration. (**A**) Representative images of scratch (wound healing) assay showing the migration of HDFs treated with CP-02 (50, 100, and 200 μg/mL) at 0, 12, 24, and 36 h. (**B**) Quantitative analysis of the percent open wound area (%) relative to the initial (0 h) wound area. Two-way ANOVA was performed to determine the statistical significance. * $p \leq 0.05$, ** $p \leq 0.01$, *** $p \leq 0.001$. Scale bar: 500 μm.

3.4. Transcriptional Analysis of CP-02-Exposed HDFs

Evaluation of the transcriptional profiling of genes associated with cell cycle regulation, growth factors, inflammation, and antioxidant defense in HDFs revealed distinct dose- and time-dependent responses following CP-02 exposure (Figure 2).

Among cell cycle regulators, *CCND1* expression was significantly upregulated at both 12 and 24 h post treatment with 100 μg/mL (3.5-fold and 4.6-fold, respectively; $p < 0.05$) and 200 μg/mL (3.3-fold [$p < 0.01$] and 3.8-fold [$p < 0.05$], respectively). In contrast, *CDKN1B* expression was markedly downregulated (0.5-fold; $p < 0.01$) at 12 h for both concentrations, returning to the basal level by 24 h with only a minor upregulation (0.8-fold) observed at 200 μg/mL at 24 h. *MYC* expression was increased in a dose-dependent manner, showing prominent upregulation at 200 μg/mL (4.2- and 2.9-folds at 12 and 24 h, respectively; $p < 0.05$), whereas the 100 μg/mL dose showed less than 2-fold induction.

Among growth factor genes, *FGF2* expression was significantly upregulated at 12 h following treatment at 200 μg/mL (2.7-fold; $p < 0.05$) but returned to basal level at 24 h for both doses. *EFG* expression was significantly upregulated in the 200 μg/mL group at 12 (5.9-fold; $p < 0.001$) and 24 h (3.6-fold; $p < 0.05$), while the lower dose induced only modest changes (<2.5-fold). No significant modulation of *TGFβ1* expression was

detected at either concentration at any time point. *VEGFA* expression modestly increased at 12 h with 100 µg/mL group (1.9-fold; $p < 0.05$) but remained below a 2-fold threshold across all conditions. Regarding inflammatory and antioxidant responses, *IL-8* expression was significantly upregulated (3.3-fold; $p < 0.05$) at 12 h in the 200 µg/mL group and modestly increased (1.6-fold) at 100 µg/mL, with both returning to basal levels at 24 h. *CAT* expression was modestly induced (<1.5-fold) at 12 h with both doses but remained at basal levels at 24 h.

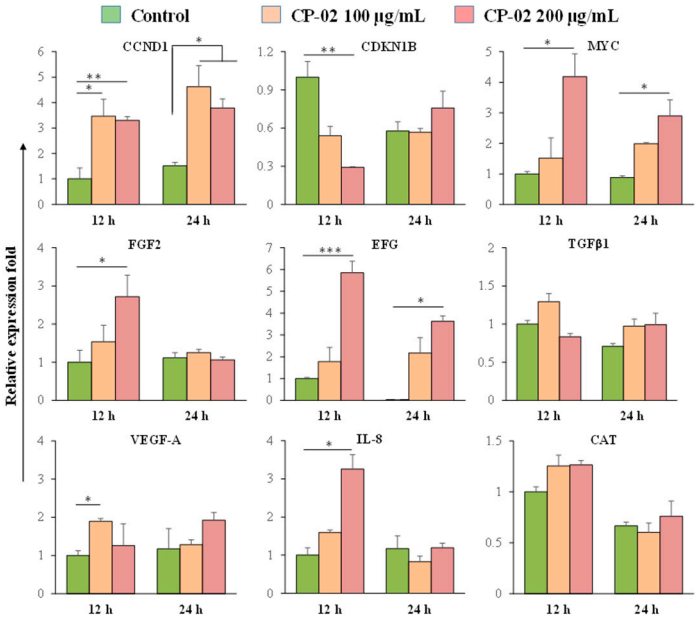

Figure 2. Relative mRNA expression levels in HDFs treated with CP-02 (100 and 200 µg/mL) for 24 and 48 h. qRT-PCR was performed on total RNA from HDFs. All Ct values were corrected for the efficiency of the respective primer sets in relation to the *GAPDH* housekeeping gene. The statistically significant difference was determined using an unpaired two-tailed t-test between the control and CP-02-treated groups, * $p \leq 0.05$, ** $p \leq 0.01$, and *** $p \leq 0.001$.

3.5. Effect of CP-02 on Amputated Larval Caudal Fin Regeneration

The regenerative potential of CP-02 was evaluated using a caudal fin amputation model in zebrafish larvae, with regeneration assessed by measuring fin fold length and growth area over time. Initial toxicity screening revealed that CP-02 concentrations above 6.5 µg/mL significantly increased embryonic mortality and caused visible deformities, including yolk sac edema (YSE), head malformations (HMs), and axial malformations (AMs) (Supplementary Figure S3A,B). The median lethal dose (LD_{50}) was determined to be 6.8 µg/mL. Based on this toxicity profile, two non-lethal concentrations, 2.5 and 5 µg/mL, were selected for regenerative analysis. Both concentrations of CP-02 (2.5 and 5 µg/mL) demonstrated a time-dependent increase in fin fold length and growth area at 24, 48, and 72 hpa, compared to control larvae (Figure 3A,B). At 48 hpa, the 5 µg/mL CP-02-treated group showed a significantly greater fin growth area (2.6 mm^2) compared to the control group (1.1 mm^2; $p < 0.05$), indicating accelerated regeneration. At 72 hpa, both treatment groups exhibited significantly enhanced growth areas (2.5 µg/mL: 3.7 mm^2; 5 µg/mL: 3.5 mm^2; $p < 0.001$) (Figure 3C). Similarly, fin fold length was increased in both CP-02-treated groups (2.5 and 5 µg/mL) compared with that in the control at 48 and 72 hpa. In particular, larvae exposed to a higher dose (5 µg/mL) showed a significant increase (0.2 mm) compared to the control (0.07 mm) at 72 h ($p < 0.05$).

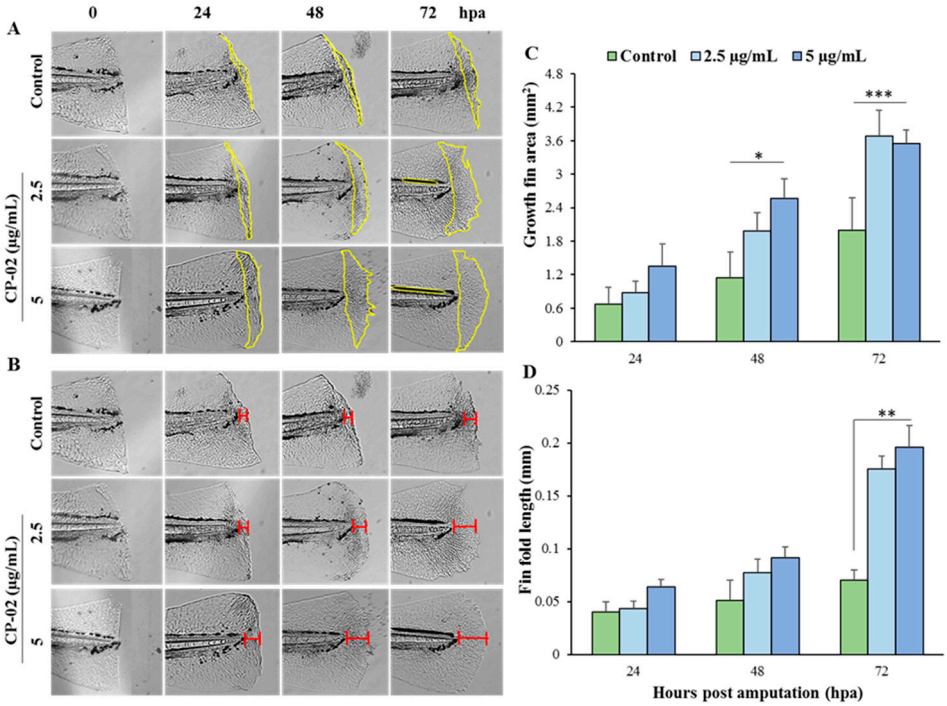

Figure 3. Effect of CP-02 exposure on caudal fin regeneration in larval zebrafish. Zebrafish larvae caudal fin primordia (92 hpf) were surgically ablated just posterior to the notochord. After amputation, larvae were exposed to CP-02 (2.5 and 5 µg/mL) or vehicle control (NF water). The images show the larval (**A**) growth fin (marked in yellow margin) and (**B**) fin fold length (marked in red line)in each group. Quantitative analysis measured individual fin data using ImageJ software and expressed (**C**) growth fin area and (**D**) fin fold length. Error bars represent means ± standard error of means (SEM). Two-way ANOVA followed by Dunnett's post hoc test was performed for statistical significance. * $p \leq 0.05$, ** $p \leq 0.01$, and *** $p \leq 0.001$.

3.6. Effect of CP-02 Intramuscular Adminstration on Wound Healing

The effect of CP-02 in promoting dermal wound healing was assessed using a full-thickness wound model in adult zebrafish. Wounds were created on the dorsolateral muscle, and four doses of CP-02 were administrated to the dorsal muscle of the left side of the fish, targeting distinct phases of wound healing, including inflammation, granulation, and remodeling (Figure 4A). Initial wound assessment revealed that wound diameter expanded during the early inflammatory phase. On average, wounds created on day 0 measured 2.7 ± 0.08 mm and increased to 3.6 ± 0.12 mm by 2 dpw, primarily due to inflammation). The CP-02- and EGF-treated groups displayed visible inflammatory responses by 2 dpw, while similar signs were delayed until 4 dpw in the vehicle-treated group (Figure 4B). In the CP-02 and EGF groups, wound margins showed progressive pigment restoration and contraction beginning on 4 dpw, unlike the vehicle group. Wound margins were visible in most of the fish in the three groups with the maximum wound size on 2 dpw; hence, the first quantification of wound size was performed on 2 dpw, with subsequent measurements used to calculate the healed area (%) and healing rate (% per day). The CP-02 group showed a higher healed area (%) than the EGF and control groups on 12 and 16 dpw. Compared with those in the vehicle group, healed area% increased in the CP-02 group on both 12 and 16 dpw (58.7% vs. 35.0%; $p < 0.05$ and 76.0% vs. 43.6%; $p < 0.01$, respectively) (Figure 4C). The EGF group also showed a significantly increased healed area% on only 16 dpw (70.8%) compared with the vehicle group. The healing rate was also increased in both the CP-02 and EGF groups compared with that in the vehicle group for all the considered time points (Figure 4D). However, WHR was increased significantly in the CP-02 group (39.5%/day) compared with that in the control group (25.0%/day) on 12 dpw ($p < 0.05$).

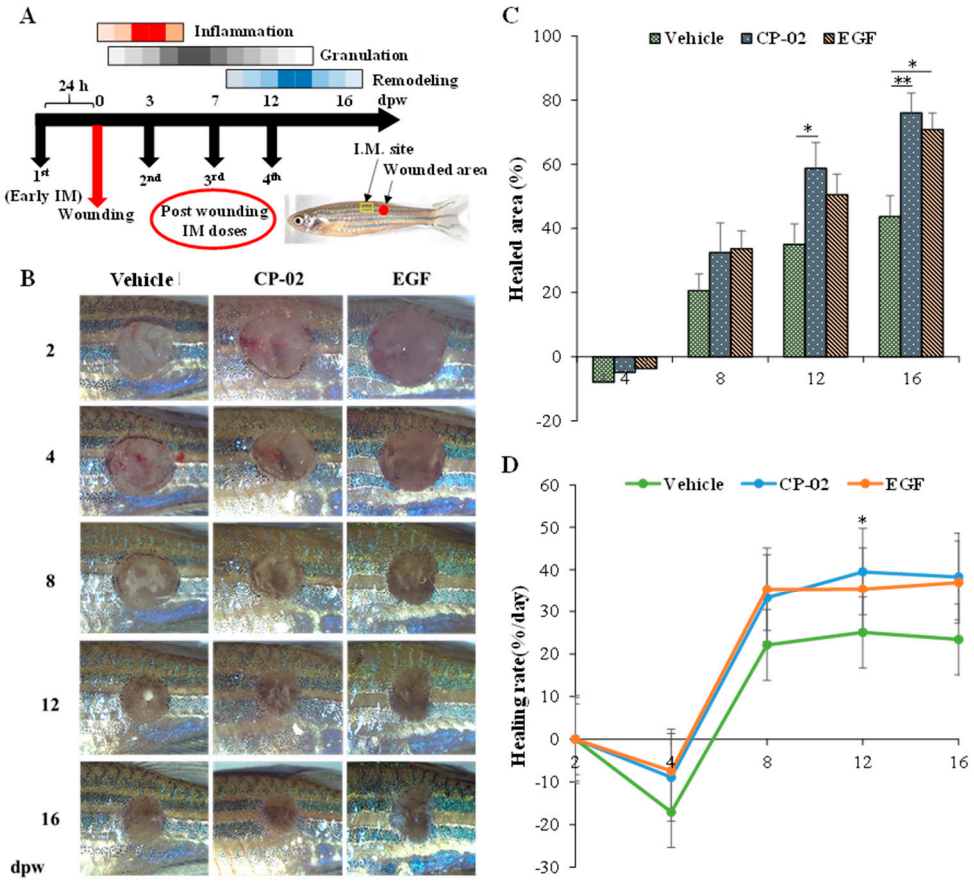

Figure 4. Representative images showing the (**A**) CP-02 treatment (IM) design targeting the three main wound healing phases (inflammation, granulation, and remodeling), (**B**) wound site of the control, CP-02, and EGF groups. Graphs showing the (**C**) healed area (%) and (**D**) wound healing rate (%/day). The healed area was calculated each day based on a wound size of 2 dpw. Error bars represent means ± standard deviation (SD). Statistical significance was determined using two-way ANOVA followed by Bonferroni post-tests (* $p \leq 0.05$, ** $p \leq 0.01$, n = 12).

3.7. Histological Assessment of the Wound Healing Effects of CP-02

Histological analysis was performed to confirm the wound healing effect of CP-02 using wounded muscle tissues on 7 and 12 dpw. Key parameters evaluated included inflammatory cell infiltration, granulation, scab appearance, identification of the neo-epidermal layers (dermal and epidermal), and re-epithelialization at the wound site. Zebrafish skin comprises three main layers: outer epidermis, inner dermis (including scales), and subcutaneous adipocytes with muscle tissue. Histological sections revealed that the inflicted deep wounds resulted in the complete removal of the epidermis and dermis, with slight damage extending to the muscle tissue. On 7 dpw, both CP-02- and EGF-treated groups showed dense granulation tissues at the wound bed with a thin multicellular neo-epidermis (Figure 5A). In contrast, the vehicle group showed incomplete granulation, persistent scab formation from damaged epithelial tissues, and a higher infiltration of inflammatory cells compared with the CP-02 and EGF groups on 7 dpw. By 12 dpw, CP-02-treated tissues demonstrated significant progress in tissue regeneration. The epidermal and dermal layers were well reconstituted, with granulation tissue largely replaced by collagen deposition within the underlying muscle. In contrast, the vehicle group exhibited delayed healing, characterized by an indistinct neo-epidermis and residual tissue damage at the wound bed. Semi-quantitative histological scoring further confirmed these findings, with CP-02 treatment resulting in higher granulation and re-epithelialization scores and reduced inflammatory cell infiltration and scab formation compared to the vehicle group (Figure 5B).

A

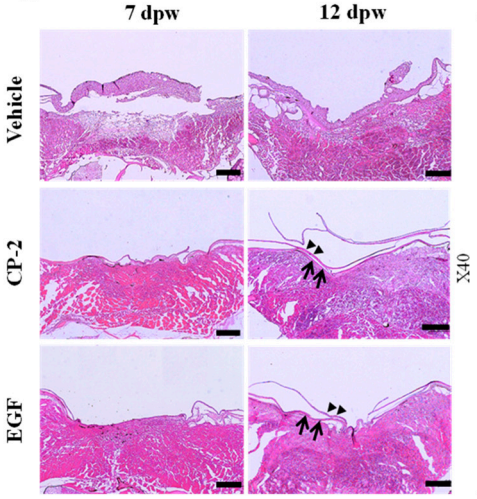

B

dpw	Histological parameter	Groups		
		Vehicle	CP-02	EGF
7	Inflammatory cell infiltration	+++	++	++
	Scab	+++	-	-
	Granulation tissue	+	+++	++
	Re-epithelialization	-	++	+
12	Inflammatory cell infiltration	++	+	+
	Scab	++	-	-
	Granulation tissue	++	+++	+++
	Re-epithelialization	+	+++	++

Figure 5. Histological Assessment of the Wound Healing Effects of CP-02. (**A**) Representative images of H&E-stained zebrafish wounded muscle tissues are marked as newly formed epidermis (black arrowheads) and dermis (black arrows). (**B**) Semi-quantitatively analyzed major histological parameters (inflammatory cell infiltration, scab, granulation tissues, and re-epithelialization) demonstrating the wound inflammation, removing the damaged tissues (scab), and re-epithelization on wound surface on 7 and 12 dpw. Notes: +, slight; ++, moderate; +++, marked; -, absence. Scale bar: 500 μm.

3.8. Analysis of Transcriptional Profile of CP-02

To further elucidate the molecular mechanisms underlying CP-02-mediated wound healing, qRT-PCR was performed on wounded muscle tissues on 4 and 12 dpw. The analysis focused on the expression of genes associated with inflammation (*tnf-α*, *il1-β*, and *il-10*), ECM remodeling (*tgfb1*, *mmp9*, *mmp13*, and *timp2b*), and scar formation (*acta2*, *ctgfb*, *cdh1*, and *col9a3*) (Figure 6). On 4 dpw, CP-02 significantly increased the expression of *tnf-α* (4.7-fold; $p < 0.01$) compared to the vehicle and EGF groups (1.7-fold). However, *tnf-α* expression was the highest in the vehicle group on 12 dpw, while it was suppressed in both the CP-02 and EGF groups (<1.0-fold). Expression of *il1-β* was significantly upregulated in the CP-02 (4.2-fold; $p < 0.001$) and EGF (3.3-fold; $p < 0.01$) groups, whereas that of *il-10* was increased in the CP-02 group (3.0-fold) compared with that in the vehicle groups. However, *il1-β* and *il-10* were the highest in the vehicle groups on 12 dpw, whereas they were downregulated in both the treatment groups (<1.0-fold). CP-02 treatment led to marked upregulation of *tgfb1*, *mmp9*, and *mmp13* compared with that in the vehicle and EGF groups on 4 dpw. Expression of *tgfb1* and *mmp9* increased in the CP-02 (3.5- and 4.8-fold, respectively) and EGF (1.8- and 1.3-fold, respectively) groups compared with that in the vehicle group. Similarly, *mmp13* levels were elevated in both the CP-02 (4.4-fold) and EGF (2.4-fold) groups on 4 dpw compared with that in the control group. Moreover, on 12 dpw, vehicle-treated tissues showed the highest expression of *tgfb1* (1.5-fold) and *mmp13* (3.5-fold), whereas the CP-02 and EGF groups showed downregulated or stable levels, except for *mmp13*, which remained elevated in CP-02 (4.7-fold). The levels of *acta2* increased significantly ($p < 0.05$) in the CP-02-treated group (6.5-fold) on 4 dpw; however, its expression was slightly upregulated (2.3-fold; $p > 0.05$) compared with that in the control group. In contrast, the expression level of *ctgfb* was suppressed (<0.2-fold) in both treatment groups (CP-02 and EGF) on 4 dpw. The expression level of *cdh1* was significantly increased in the EGF (38.2-fold) group compared with that in the vehicle and CP-02 (3.9-fold) on 4 dpw. Expression of *col9a3* was slightly enhanced in the CP-02 group (1.8-fold) on 4 dpw compared with that in the vehicle and EGF groups. Expression levels of *acta2*, *ctgfb*, *cdh1*,

and *col9a3* also increased in the vehicle group on 12 dpw compared with those in the other treatment groups (CP-02 and EGF).

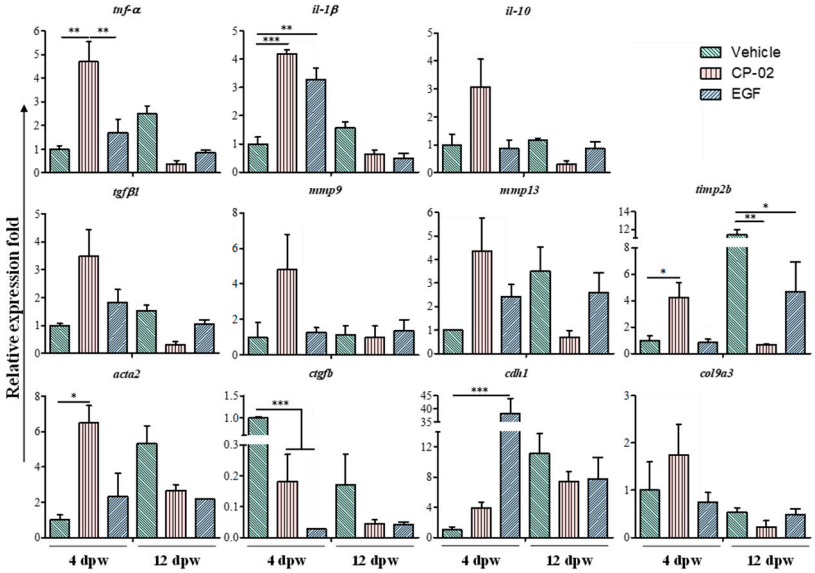

Figure 6. Summary of mRNA expression in wounded muscle tissues on 4 and 12 dpw. Gene expressions were selected based on inflammatory responses, extracellular matrix remodeling, and excess scar formation in a healing wound. The mRNA expression levels of each gene were normalized to that of the β-actin mRNA level, and folds were analyzed using the $2^{-\Delta\Delta CT}$ method. Statistical significance was determined using two-way ANOVA followed by Bonferroni post-tests (* $p \leq 0.05$, ** $p \leq 0.01$, *** $p \leq 0.001$, n = 3).

4. Discussion

Wound healing remains a complex clinical challenge that depends on tightly coordinated cellular signaling to drive proliferation, granulation, and neovascularization following injury [16–18]. Pharmacological approaches targeting growth factors, cytokines, and immunoregulatory pathways have shown the potential to enhance the healing process [19,20]. However, systemic administration of these drugs is often associated with limited efficacy, adverse effects, and high costs. Consequently, there is a critical need for novel, efficient biomaterials with improved therapeutic potential. Recent advances in bioactive peptides have increased interest in their therapeutic applications, particularly in wound healing and skin regeneration [21–23]. These peptides exhibit high bioactivity, specificity, and stability, making them attractive candidates for biopharmaceutical development. CPs are widely incorporated into cosmetic formulations due to their regenerative, anti-wrinkling, and anti-aging properties [9].

Based on its rich amino acid composition, including aspartate, alanine, and arginine, CP-02 demonstrates high hydrophilicity. In vitro toxicity analysis revealed an IC_{50} of 322 μg/mL in HDFs, indicating a broad therapeutic window of CP-02. Notably, CP-02 enhanced cell viability at concentrations ranging from 100 to 250 μg/mL, possibly through stimulating fibroblast proliferation. Furthermore, in vitro wound healing assays confirmed that CP-02 effectively promote HDF migration and proliferation.

Gene expression analysis revealed increased levels of *CCND1* and *MYC* in CP-02-treated cells at both doses. *CCND1* forms a complex with cyclin-dependent kinases (Cdk)4/6 to facilitate cellular adhesion and migration [24]. Enhanced *MYC* expression regulates multiple cellular processes, including proliferation, differentiation, and apoptosis in human cells [25]. Together these findings suggest that CP-02 beneficially modulates key cell cycle regulatory genes to enhance cellular migration and proliferation.

Furthermore, we observed the upregulation of wound healing-related growth factors, including *FGF2*, *EGF*, and *VEGFA*, at the mRNA level, further supporting the role of CP-02 in promoting tissue repair. FGF2 is known for its ability to enhance cell growth and facilitate wound healing [26,27]. EGF plays an important role in wound healing by enhancing fibronectin mRNA and protein levels in HDFs [28]. Moreover, VEGFA production by stromal fibroblasts plays a key role in angiogenic properties [29].

Together, these findings demonstrate that CP-02 promotes HDF proliferation and migration in vitro by upregulating *EGF2*, *EGF*, and *VEGFA*. CP-02 also appeared to exert early anti-inflammatory effects by modulating IL-8 expression in HDFs, although further mechanistic studies are needed to confirm this.

Studies have shown that low-molecular-weight signal peptides (<500 Da) can penetrate the skin barrier and stimulate the synthesis of collagen, elastin, proteoglycan, and fibronectin in the ECM [9,30]. Although CP-02 has a molecular weight of 892.9 Da, exceeding the typical threshold, it still demonstrated significant regenerative effects in a zebrafish model, which is widely used for evaluating toxicity, regeneration, and wound healing due to its transparency and rapid developmental processes [12,31,32]. Furthermore, previous studies have shown that regeneration analyses in zebrafish larvae at 96 hpf provide advantages over adult fish due to their anatomical simplicity, avascular fin structures, and rapid regenerative capacity [12,33]. Consistently, our in vivo data revealed accelerated fin regrowth following CP-02 treatment, as evidenced by the quantification of fin area and fold length from 24 to 72 hpa in a dose-dependent manner. At the highest concentration tested (5 μg/mL), CP-02 enabled complete restoration of fin shape and size by 72 hpa. Anatomically, the larval fin consists a mesenchymal core comprising fibroblast-like cells, nerves, and actinotrichia, surrounded by a bilayered epidermis made of p63-positive keratinocytes [32]. We hypothesize that CP-02 enhances epidermal regeneration by stimulating the proliferation of fibroblasts and keratinocytes, thereby promoting the formation of a blastema-like structure necessary for efficient tissue restoration. Additionally, CP-02 exhibits a broader therapeutic range than other synthetic peptides, such as antimicrobial [34] and host-defense [35] peptides. Collectively, these findings suggest the robust therapeutic potential of CP-02.

We further validated the skin regeneration potential of CP-02 using a wounded zebrafish model, in which CP-02 was systemically administered via I.M. injection. In addition to evaluating its wound healing efficacy, this model allowed us to assess key properties of CP-02, including peptide stability, reactivity, toxicity, and overall therapeutic potential. A single dose of CP-02 was administered to promote early re-epithelialization and establish a balanced cytokine profile following injury, followed by three additional doses targeting the granulation and tissue remodeling phases of wound healing. According to Sveen et al., zebrafish wounds undergo distinct healing stages: early re-epithelialization, granulation (2–15 dpw), and remodeling beginning around 7 dpw [36]. Epidermal keratinocytes mediate re-epithelialization, while granulation tissue provides a provisional ECM that supports the activation and recruitment of fibroblasts, inflammatory cells, endothelial cells, and myofibroblasts [37]. Morphological analysis revealed that CP-02 treatment reduced inflammation, accelerated tissue regeneration, and decreased scar formation compared to the vehicle control from 2 to 16 dpw. These effects were also compared to a positive control group with exogenous EGF (I.M.). Both CP-02 and EGF promoted rapid re-epithelialization; however, CP-02 elicited lower inflammatory responses during the early healing stage (2 dpw). The percentage of healed area and the overall healing rate were significantly greater in the CP-02 group than that in the vehicle group.

Histological validation was performed using H&E staining of muscle tissues collected during peak granulation (7 dpw) and remodeling (12 dpw) stages. At 7 dpw, sections from

both CP-02 and EGF groups showed complete granulation tissue formation with minimal inflammatory cell infiltration compared to the vehicle group. By 12 dpw, remodeled tissues exhibited well-differentiated dermal and epidermal layers, degradation of the provisional ECM, and the formation of new muscle tissues in both treatment groups.

To understand the molecular effects of CP-02 on zebrafish wound healing, we analyzed transcriptional responses related to cytokine signaling, growth factor expression, and scar formation at key phases of healing, specifically the inflammatory (4 dpw) and remodeling (12 dpw) phases. During the inflammatory phase, pro-inflammatory cytokines, such as TNF-α and IL-1, initiate provisional ECM formation by promoting the expression of MMPs [5,38]. These cytokines can also induce the production of additional growth factors, thereby indirectly promoting re-epithelialization [5]. Our data showed elevated expression of both *tnf-α* and *il-1β* in the CP-02 group compared with the vehicle- and EGF-treated groups on 4 dpw. Similarly, expression of *il-10*, an anti-inflammatory cytokine, was also increased in the CP-02-treated group, indicating balanced pro- and anti-inflammatory profiles. TGF-β1 is a key growth factor throughout all healing phases and promotes the recruitment of additional inflammatory cells, angiogenesis, and re-epithelialization [5]. In this study, *tgfb1* was upregulated in both the CP-02 and EGF groups compared with the vehicle group. Enzymatic activation of MMP-9 (gelatinases) and MMP-13 (collagenases) has been shown to promote wound healing through degradation of the ECM, enhancing cell migration, epithelial regeneration, tissue granulation, and wound contraction [38]. However, excessive expression of MMP-9 and MMP-13 can impair cell attachment to the ECM and induce pathologic destruction of connective tissue at the wound site [38,39]. Tissue inhibitors of MMPs (TIMPs), which are natural inhibitors of MMPs, are also involved in regulating the inflammatory response [39]. In our data, the highest expression of *mmp9*, *mmp13*, and *timp2b* was observed in the CP-02-0treated group at 4 dpw, whereas, their expression was lowest at 12 dpw. During the remodeling stage, the CP-02 and EGF groups showed reduced *timp2b* levels, consistent with reduced inflammation and ECM resolution. These findings suggest that CP-02 enhances wound healing by modulating MMPs and their inhibitors, thereby regulating cytokine signaling, cell adhesion, and ECM turnover.

Furthermore, CP-02 demonstrated strong potential to stimulate cytokine production, cellular responses, and expression of growth factors that promote rapid re-epithelialization and granulation during wound healing. Previous studies have shown that topical signal and carrier peptides can promote anti-aging, anti-wrinkle, skin renewal, and hair growth activities by modulating collagen production [9]. Understanding the molecular basis of scarless wound healing is also important for developing CPs. Following injury, skin regeneration and scarring are considered physiologically opposing outcomes in scarless healing [40]. To evaluate this, we analyzed the expression of major scar-/or fibrosis-related genes, including *acta2*, *ctgfb*, *cdh1*, and *col9a3*, in zebrafish wounded muscles. The findings showed that *acta2* and *cdh1* were significantly upregulated in the CP-02 and EGF groups on 4 dpw, compared with the vehicle group. Consistent with these findings, previous studies in rodent models have demonstrated that Acta2 enhances myofibroblast motility, wound contraction, and signaling regulation during wound healing [41]. In zebrafish, *cdh1* plays a key role in regulating cell motility and tissue organization during early development [42]. Connective tissue growth factor (CTGF) is expressed during various tissue growth and development processes [43]; however, treatment with CP-02 or EGF suppressed *ctgfb* expression in wounded tissues on 4 dpw. In zebrafish, *col9a3* has been extensively studied for its role in cartilage development and collagen synthesis [44]. Studies have revealed that collagen III, produced during the proliferative phase, is subsequently replaced by the stronger collagen I during the remodeling phase [45]. In the present study, *col9a3* was

upregulated in the CP-02 at 4 dpw, suggesting its involvement in ECM development during the early stage of healing.

Furthermore, all scar-associated genes were downregulated at 12 dpw in both the CP-02 and EGF groups compared with the vehicle group. These findings confirm that CP-02 enhances collagen synthesis by modulating multiple signaling pathways during the early healing phase while suppressing excessive collagen production during remodeling to reduce scar formation. Overall, our results demonstrate that I.M. administration of CP-02 accelerates re-epithelialization and granulation, promoting rapid wound healing while minimizing scar-related complications.

5. Conclusions

In this study, we synthesized the peptide CP-02 (sequence: CDARSDAR) and demonstrated its potent wound healing and regenerative properties in both in vitro and in vivo models. CP-02 significantly enhanced HDF migration and upregulating key transcriptional markers associated with the cell cycle, growth factors, and cytokine signaling. The regenerative potential of CP-02 was further validated in zebrafish larvae, where it promoted dose-dependent fin regeneration from 24 to 72 hpa. In adult zebrafish, I.M. administration of CP-02 accelerated wound closure, facilitated rapid re-epithelialization, and supported balanced cytokine and growth factor expression. Importantly, CP-02 also reduced excessive fibrotic gene expression during the remodeling phase, highlighting its potential to minimize scar formation and improve overall tissue repair. However, the advantages of CP-02 extend beyond its efficacy. CP-02 is structurally simple and amenable to scalable synthesis, making it potentially more cost-effective than peptides that require complex chemical modifications or recombinant production. Together, its potent biological activity, favorable healing kinetics, and ease of manufacturability position CP-02 as a promising and economically viable candidate within the growing landscape of peptide-based wound healing therapies.

Overall, CP-02 could be considered a multifunctional pro-healing agent, particularly suited for integrating platforms such as peptide-based hydrogels. In the future, this peptide could be encapsulated within exosomes or other biomaterial-based delivery systems to enable sustained release and enhanced immunomodulatory effects. Such advanced formulations may further amplify its therapeutic potential in wound healing applications.

Supplementary Materials: The following supporting information can be downloaded at https://www.mdpi.com/article/10.3390/cosmetics13010016/s1: Figure S1: Final purity and molecular weight of synthesized CP-02. Figure S2: In vitro cytotoxicity of CP-02 on HDFs. Figure S3: In vivo toxicity of CP-02 exposed with zebrafish embryos. Table S1: Description of primers used in this study.

Author Contributions: Conceptualization, S.L.E. and M.D.Z.; formal analysis, S.L.E.; funding acquisition, M.D.Z.; investigation, C.N. and S.L.E.; methodology, C.N., S.L.E. and M.D.Z.; project administration, M.D.Z.; resources, M.D.Z.; supervision, M.D.Z.; writing—original draft, S.L.E.; writing—review and editing, C.N., S.L.E. and M.D.Z. All authors have read and agreed to the published version of the manuscript.

Funding: This work was supported by National Research Foundation of Korea (NRF) grants, funded by the Korean government (MSIT) (2023R1A2C1006901) and a research fund from Chungnam National University (2022-0716-01).

Institutional Review Board Statement: All experiments with zebrafish were conducted in accordance with the approved guidelines and regulations of the Animal Ethics Committee of Chungnam National University (Approval Code: 202109A-CNU-121, Approval Date 1 October 2021).

Informed Consent Statement: Not applicable.

Data Availability Statement: The data are available from the corresponding author upon request.

Conflicts of Interest: The authors declare no conflicts of interest.

References

1. Fields, K.; Falla, T.J.; Rodan, K.; Bush, L. Bioactive Pevptides: Signaling the Future. *J. Cosmet. Dermatol.* **2009**, *8*, 8–13. [CrossRef] [PubMed]
2. Nguyen, H.L.T.; Trujillo-Paez, J.V.; Umehara, Y.; Yue, H.; Peng, G.; Kiatsurayanon, C.; Chieosilapatham, P.; Song, P.; Okumura, K.; Ogawa, H.; et al. Role of antimicrobial peptides in skin barrier repair in individuals with atopic dermatitis. *Int. J. Mol. Sci.* **2020**, *21*, 7607. [CrossRef] [PubMed]
3. Song, Y.; Wu, C.; Zhang, X.; Bian, W.; Liu, N.; Yin, S.; Yang, M.; Luo, M.; Tang, J.; Yang, X. Short peptide potentially promotes the healing of skin wound. *Biosci. Rep.* **2019**, *39*, BSR20181734. [CrossRef]
4. Steed, D.L. The role of growth factors in wound healing. *Surg. Clin. N. Am.* **1997**, *77*, 575–586. [CrossRef] [PubMed]
5. Barrientos, S.; Stojadinovic, O.; Golinko, M.S.; Brem, H.; Tomic-Canic, M. Growth Factors and Cytokines in Wound Healing. *Wound Repair Regen.* **2008**, *16*, 585–601. [CrossRef]
6. Guo, S.; DiPietro, L.A. Critical review in oral biology & medicine: Factors affecting wound healing. *J. Dent. Res.* **2010**, *89*, 219–229. [CrossRef]
7. Carter, T.; Qi, G.; Wang, W.; Nguyen, A.; Cheng, N.; Ju, Y.M.; Lee, S.J.; Yoo, J.J.; Atala, A.; Sun, X.S. Self-Assembling Peptide Solution Accelerates Hemostasis. *Adv. Wound Care* **2021**, *10*, 191–203. [CrossRef]
8. Tang, J.; Liu, H.; Gao, C.; Mu, L.; Yang, S.; Rong, M.; Zhang, Z.; Liu, J.; Ding, Q.; Lai, R. A Small peptide with potential ability to promote wound healing. *PLoS ONE* **2014**, *9*, e92082. [CrossRef]
9. Schagen, S.K. Topical peptide treatments with effective anti-aging results. *Cosmetics* **2017**, *4*, 16. [CrossRef]
10. Linder, J. The science behind peptides. *Plast. Surg. Nurs.* **2012**, *32*, 71–72. [CrossRef]
11. el Hadmed, H.H.; Castillo, R.F. Cosmeceuticals: Peptides, proteins, and growth factors. *J. Cosmet. Dermatol.* **2016**, *15*, 514–519. [CrossRef]
12. Edirisinghe, S.; Rajapaksha, D.; Nikapitiya, C.; Oh, C.; Lee, K.-A.; Kang, D.-H.; De Zoysa, M. *Spirulina maxima* derived marine pectin promotes the in Vitro and in Vivo regeneration and wound healing in zebrafish. *Fish Shellfish. Immunol.* **2020**, *107*, 414–425. [CrossRef] [PubMed]
13. Edirisinghe, S.; Dananjaya, S.; Nikapitiya, C.; Liyanage, T.; Lee, K.-A.; Oh, C.; Kang, D.-H.; De Zoysa, M. Novel pectin isolated from *Spirulina Maxima* enhances the disease resistance and immune responses in zebrafish against *Edwardsiella piscicida* and *Aeromonas hydrophila*. *Fish Shellfish. Immunol.* **2019**, *94*, 558–565. [CrossRef] [PubMed]
14. Rajapaksha, D.C.; Edirisinghe, S.L.; Nikapitiya, C.; Dananjaya, S.; Kwun, H.-J.; Kim, C.-H.; Oh, C.; Kang, D.-H.; De Zoysa, M. *Spirulina maxima* derived pectin nanoparticles enhance the immunomodulation, stress tolerance, and wound healing in zebrafish. *Mar. Drugs* **2020**, *18*, 556. [CrossRef]
15. Livak, K.J.; Schmittgen, T.D. Analysis of relative gene expression data using real-time quantitative PCR and the $2^{-\Delta\Delta CT}$ method. *Methods* **2001**, *25*, 402–408. [CrossRef]
16. Wilkinson, H.N.; Hardman, M.J. Wound healing: Cellular mechanisms and pathological outcomes: Cellular mechanisms of wound repair. *Open Biol.* **2020**, *10*, 200223. [CrossRef]
17. Tottoli, E.M.; Dorati, R.; Genta, I.; Chiesa, E.; Pisani, S.; Conti, B. Skin wound healing process and new emerging technologies for skin wound care and regeneration. *Pharmaceutics* **2020**, *12*, 735. [CrossRef] [PubMed]
18. Frykberg, R.G.; Banks, J. Challenges in the treatment of chronic wounds. *Adv. Wound Care* **2015**, *4*, 560–582. [CrossRef]
19. Larouche, J.; Sheoran, S.; Maruyama, K.; Martino, M.M. Immune regulation of skin wound healing: Mechanisms and novel therapeutic targets. *Adv. Wound Care* **2018**, *7*, 209–231. [CrossRef]
20. Whittam, A.J.; Maan, Z.N.; Duscher, D.; Wong, V.W.; Barrera, J.A.; Januszyk, M.; Gurtner, G.C. Challenges and opportunities in drug delivery for wound healing. *Adv. Wound Care* **2016**, *5*, 79–88. [CrossRef]
21. Ting, D.S.J.; Beuerman, R.W.; Dua, H.S.; Lakshminarayanan, R.; Mohammed, I. Strategies in translating the therapeutic potentials of host defense peptides. *Front. Immunol.* **2020**, *11*, 983. [CrossRef]
22. Pfalzgraff, A.; Brandenburg, K.; Weindl, G. Antimicrobial peptides and their therapeutic potential for bacterial skin infections and wounds. *Front. Pharmacol.* **2018**, *9*, 281. [CrossRef]
23. Hong, Y.; Shim, H.; Kim, S.; Choi, N.; Kim, J.; Hwang, J.; Yun, J.; Kwon, B. The effects on dermal wound healing using novel peptide modified by bone morphogenic protein-2. *Tissue Eng. Regen. Med.* **2014**, *11*, 397–404. [CrossRef]
24. Li, Z.; Wang, C.; Jiao, X.; Lu, Y.; Fu, M.; Quong, A.A.; Dye, C.; Yang, J.; Dai, M.; Ju, X.; et al. Cyclin D1 regulates cellular migration through the inhibition of thrombospondin 1 and ROCK signaling. *Mol. Cell Biol.* **2006**, *26*, 4240–4256. [CrossRef] [PubMed]
25. Henriksson, M.; Lüscher, B. Proteins of the Myc network: Essential regulators of cell growth and differentiation. *Adv. Cancer Res.* **1996**, *68*, 109–182. [CrossRef] [PubMed]

26. Jimenez, S.K.; Sheikh, F.; Jin, Y.; Detillieux, K.A.; Dhaliwal, J.; Kardami, E.; Cattini, P.A. Transcriptional regulation of FGF-2 gene expression in cardiac Myocytes. *Cardiovasc. Res.* **2004**, *62*, 548–557. [CrossRef] [PubMed]
27. Ortega, S.; Ittmann, M.; Tsang, S.H.; Ehrlich, M.; Basilico, C. Neuronal defects and delayed wound healing in mice lacking fibroblast growth factor 2. *Proc. Natl. Acad. Sci. USA* **1998**, *95*, 5672–5677. [CrossRef]
28. Mimura, Y.; Ihn, H.; Jinnin, M.; Asano, Y.; Yamane, K.; Tamaki, K. Epidermal growth factor induces fibronectin expression in human dermal fibroblasts via protein kinase C δ signaling pathway. *J. Investig. Dermatol.* **2004**, *122*, 1390–1398. [CrossRef]
29. Hlatky, L.; Tsionou, C.; Hahnfeldt, P.; Coleman, C.N. Mammary fibroblasts may influence breast tumor angiogenesis via hypoxia-induced vascular endothelial growth factor up-regulation and protein expression. *Cancer Res.* **1994**, *54*, 6083–6086.
30. Gorouhi, F.; Maibach, H.I. Role of topical peptides in preventing or treating aged skin. *Int. J. Cosmet. Sci.* **2009**, *31*, 327–345. [CrossRef]
31. Cassar, S.; Adatto, I.; Freeman, J.L.; Gamse, J.T.; Iturria, I.; Lawrence, C.; Muriana, A.; Peterson, R.T.; Van Cruchten, S.; Zon, L.I. Use of zebrafish in drug discovery toxicology. *Chem. Res. Toxicol.* **2020**, *33*, 95–118. [CrossRef]
32. Mateus, R.; Pereira, T.; Sousa, S.; De Lima, J.E.; Pascoal, S.; Saúde, L.; Jacinto, A. In vivo cell and tissue dynamics underlying zebrafish fin fold regeneration. *PLoS ONE* **2012**, *7*, e51766. [CrossRef]
33. Bohaud, C.; Johansen, M.D.; Jorgensen, C.; Ipseiz, N.; Kremer, L.; Djouad, F. The role of macrophages during zebrafish injury and tissue regeneration under infectious and non-infectious conditions. *Front. Immunol.* **2021**, *12*, 707824. [CrossRef]
34. Cebrián, R.; Rodríguez-Cabezas, M.E.; Martín-Escolano, R.; Rubiño, S.; Garrido-Barros, M.; Montalbán-López, M.; Rosales, M.J.; Sánchez-Moreno, M.; Valdivia, E.; Martínez-Bueno, M.; et al. Preclinical studies of toxicity and safety of the AS-48 bacteriocin. *J. Advanc. Res.* **2019**, *20*, 129–139. [CrossRef]
35. Flagler, M.J.; Tamura, M.; Laughlin, T.; Hartman, S.; Ashe, J.; Adams, R.; Kozak, K.; Cresswell, K.; Mullins, L.; Jarrold, B.B.; et al. Combinations of peptides synergistically activate the regenerative capacity of skin cells in vitro. *Int. J. Cosmet. Sci.* **2021**, *43*, 518–529. [CrossRef] [PubMed]
36. Sveen, L.; Karlsen, C.; Ytteborg, E. Mechanical induced wounds in fish—A review on models and healing mechanisms. *Rev. Aquac.* **2020**, *12*, 2446–2465. [CrossRef]
37. Werner, S.; Krieg, T.; Smola, H. Keratinocyte–Fibroblast Interactions in Wound Healing. *J. Investig. Dermatol.* **2007**, *127*, 998–1008. [CrossRef]
38. Chakraborti, S.; Mandal, M.; Das, S.; Mandal, A.; Chakraborti, T. Regulation of matrix metalloproteinases, An overview. *Mol. Cell Biochem.* **2003**, *253*, 269–285. [CrossRef] [PubMed]
39. Gill, S.E.; Parks, W.C. Metalloproteinases and their inhibitors: Regulators of wound healing. *Int. J. Biochem. Cell Biol.* **2008**, *40*, 1334–1347. [CrossRef] [PubMed]
40. Jiang, D.; Rinkevich, Y. Scars or Regeneration?—Dermal fibroblasts as drivers of diverse skin wound responses. *Int. J. Mol. Sci.* **2020**, *21*, 617. [CrossRef]
41. Rockey, D.C.; Weymouth, N.; Shi, Z. Smooth muscle α actin (Acta2) and myofibroblast function during hepatic wound healing. *PLoS ONE* **2013**, *8*, e77166. [CrossRef] [PubMed]
42. Babb, S.G.; Marrs, J.A. E-Cadherin regulates cell movements and tissue formation in early zebrafish embryos. *Dev. Dyn.* **2004**, *230*, 263–277. [CrossRef] [PubMed]
43. Wang, Y.; Li, F.-G.; Qin, B.; Chen, J.; Jiang, X.-Y.; Zou, S.-M. Duplicated connective tissue growth factor genes in hypoxia-sensitive blunt snout bream Megalobrama amblycephala and their in vivo expression. *Comp. Biochem. Physiol. Part B Biochem. Mol. Biol.* **2015**, *181*, 42–49. [CrossRef] [PubMed]
44. He, H.; Wang, C.; Tang, Q.; Yang, F.; Xu, Y. Elucidation of possible molecular mechanisms underlying the estrogen-induced disruption of cartilage development in zebrafish larvae. *Toxicol. Lett.* **2018**, *289*, 22–27. [CrossRef]
45. Reinke, J.; Sorg, H. Wound repair and regeneration. *Eur. Surg. Res.* **2012**, *49*, 35–43. [CrossRef]

Disclaimer/Publisher's Note: The statements, opinions and data contained in all publications are solely those of the individual author(s) and contributor(s) and not of MDPI and/or the editor(s). MDPI and/or the editor(s) disclaim responsibility for any injury to people or property resulting from any ideas, methods, instructions or products referred to in the content.